RSC Advances

ROYAL SOCIETY OF CHEMISTRY

www.rsc.org/advances

Graphical Abstract:

A novel electrochemical biosensor for deoxyribonucleic acid detection based on exonuclease III assisted deoxyribonucleic acid recycling and rolling circle amplification

By **Fenglei Gao*, Yan Du, Jingwen Yao, Yanzhuo Zhang and Jian Gao**

A strategy for electrochemical detection of DNA was developed by exonuclease III assisted DNA recycling and the rolling circle amplification.

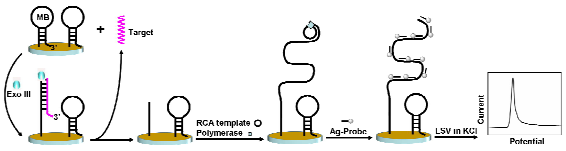

A novel electrochemical biosensor for DNA detection based on exonuclease III assisted target recycling and rolling circle amplification

Fenglei Gao*, Yan Du, Jingwen Yao, Yanzhuo Zhang, Jian Gao

Jiangsu Key Laboratory of New Drug Research and Clinical Pharmacy, School of Pharmacy, Xuzhou Medical College, 221004, Xuzhou, China.

Abstract:

We developed a novel dual amplification strategy for ultrasensitive electrochemical detection of DNA based on exonuclease III assisted target recycling and rolling circle amplification (RCA). In this assay, gold electrode was used to immobilize molecular beacon (MB) with a 3′ overhang end as recognition probe and performed the dual signal amplification procedure. In the presence of target DNA, MB hybridized with the target DNA to form a duplex region, and create 3′-blunt for Exo III to initiate the target DNA recycling amplification process to cleave numerous MB probes. Then the left MB fragment as a primer hybridized with the RCA template to initiate the RCA process. Subsequently, the detection probe modified Ag NPs hybridize with the long amplified DNA products, resulting in the multiplication of Ag NPs on the electrode surface, which were used for subsequent electrochemical strip analysis of silver. This novel signal amplification strategy could detect target DNA down to 6.4 amol L^{-1} with a dynamic range spanning 5 orders of magnitude. In addition, this method could avoid de-oxygenation procedure for usual electrochemical detection, thus had a promising application in clinical diagnosis.

Keywords: rolling circle amplification; electrochemical; silver nanoparticles; sensors;

*Corresponding author. Tel./Fax: +86-516-83262138.

Email address: jsxzgfl@sina.com.

1. Introduction

Sequence-specific detection of DNA associated with genetic or pathogenic diseases and forensic applications have become increasingly important in molecular diagnostics[1-7]. Various methods have been used to detect sequence-selective DNA, including colorimetry[8-12], electrochemical[13-18], electrochemiluminescence[19-22], field-effect transistors[23,24], and fluorescence[25-29]. Among these methods, electrochemical method has attracted particular attention because of its high sensitivity and low cost. Electrochemical detection of DNA can be accomplished by using enzyme or metal nanoparticles labels that generate an amplified signal via the production of an electroactive compound or via a bioelectrocatalytic process[30-34]. For example, many groups have reported nanoparticle-based protocol for detection of DNA based on electrochemical stripping analysis silver nanotags[33, 34]. Despite these advantages, above-mentioned DNA sensor is not sensitive enough because of that a single target molecule only reacts with a single signaling probe, limiting the total signal gain and corresponding sensitivity. Therefore, there is a great desire to improve the performance of electrochemical DNA sensors in sensitivity.

Recently, in order to improve the sensitivity of DNA detection, the strategies based on enzyme-aided signal amplification have been employed, such as polymerase chain reaction (PCR)[35-37] and nicking endonucleases[38,39] signal amplification. However, these methods demonstrate many significant flaws. For example, PCR requires expensive equipment and precise temperature control, limiting its application for low-cost DNA detection applications. Nicking endonucleases require target DNA

with a specific sequence for enzyme recognition, which limits the versatility. Target recycling achieved by exonucleases is a new method to promote signal amplification. Exonuclease III (Exo III) is a kind of exonuclease catalyzing the stepwise removal of mononucleotides from 3′-blunt termini of double-stranded DNA, which is not active on 3'-overhang ends of double-stranded DNA or single-stranded DNA[40,41]. In this method, target firstly combines with the signal probe. And then the exonucleases selectively degraded the signal probe, leading to the dissociation of the complex of target and signal probe, simultaneously. It can realize simple detection, high sensitivity and low detection limit in combination with electrochemical strategies.

This work further combined the Exo III assisted DNA recycling with rolling circle amplification (RCA) for electrochemical detection of DNA. RCA has recently attracted considerable attention due to the significant advantages of rapid and efficient analysis. In typical RCA, a long single stranded DNA (ssDNA) containing thousands of tandem repeats complementary to the circular template can be produced within 1–3 h under constant temperature. RCA has been employed for the analysis of proteins, nucleic acids, and cocaine by the combination with fluorescence[42], UV-vis spectroscopy[43] and chemiluminescence[44].

In our approach, the target DNA hybridize with the MB probes on the sensor surface and create 3′-blunt for Exo III to initiate the target DNA recycling amplification process to cleave numerous MB probes. The left MB fragment on the sensor surface is subject to in situ RCA to generate massive long DNA sequences. Using oligonucleotide functionalized Ag NPs as signal tag to bind the repeated RCA

sequences, an extremely sensitive method for electrochemical detection of DNA was thus proposed by stripping voltammetric analysis. The proposed strategy exhibits high and superior selectivity towards target DNA, which may provide a universal sensing platform for DNA-based molecular diagnostics.

2. Experimental

2.1 Reagents and materials.

Exo III, T4 DNA ligase and 10 × T_4 L DNA ligase buffer were obtained from Takara Biotechnology Co., Ltd. (Dalian, China). The DNA polymerization and deoxyribonucleoside 5′-triphosphates (dNTPs) mixture were purchased from Epicenter Technologies (Madison, WI). Human serum samples were kindly provided by the affiliated hospital of Xuzhou medical college (Xuzhou, China). Hexaammineruthenium (III) chloride (RuHex) and bovine serum albumin (BSA) was obtained from Aladdin-Reagent, Inc. (Shanghai, China). Other reagents were purchased from China National Medicines Co. Ltd. (Beijing, China). Solutions were prepared with Milli-Q deionized water.

2.2 Buffers.

DNA hybridization buffer was phosphatebuffered saline (137 mM NaCl, 2.5 mM Mg^{2+}, 10 mM Na_2HPO_4, and 2.0 mM KH_2PO_4, pH 7.4). DNA was stored in Tris-HCl (10 mM, pH 8.0) containing 1 mM ethylenediaminetetraacetic acid. Phosphate-buffered saline (PBS, 0.1 M) of various pH was prepared by mixing the stock solutions of NaH_2PO_4 and Na_2HPO_4. The washing buffer was PBS (0.1 M, pH 7.4) containing 0.05% (w/v) Tween-20. The blocking buffer was 10 mM PBS

containing 0.1 M NaCl, 0.02 % Tween-20 and 10 % BSA, pH 7.4. The ligase buffer was 66.0 mM Tris-HCl (pH 7.6), 6.6 mM $MgCl_2$, 10.0 mM dithiothreitol (DTT), and 0.1 mM adenosine triphosphate (ATP). 40.0 mM Tris–HCl buffer (pH 7.5), 50.0 mM KCl, 10.0 mM $MgCl_2$, 5.0mM $(NH_4)_2SO_4$, and 4.0 mM DTT formed RCA reaction buffer.

The oligonucleotides were purchased from Sangon Biological Engineering Technology & Co. Ltd. (Shanghai, China) and purified using high-performance liquid chromatography.

MB: 5′-SH-CGTACCACAACAGCATGGTACGCGCCAATATTTACGTGCTG CTATGGTACGAGTTC-3′,

Target: 5′-GAACTCGTACCATAGCAGCACGTAAATATTGGCGTATT-3′,

Single-base mismatched target: 5′-GAACTCGTACCATAGCAGCTCGTAAATAT TGGCGTATT-3′,

Non-complementary: 5′-TGGCATCTTCACCTTGACATGACATACAGTTGAA TGAT-3′,

Padlock probe: 5′-p-ATGCTGACTAACGGTGGCCGGTTGAAATTCAGTCGGCT TCGAATGCGTACC-3′,

Primer: 5′-AAACAGCATGGTACG-3′,

Detection probe: 5′-SH-CGGTTGAAATTCAGT-3′.

Fluorescent probe: 5′-FAM-AGCTACTGCCGGTTGAAATTCAGTAGTAGCT-BHQ-3′

2.3 Preparation of detection probe-modified Ag NPs.

A suspension of citrate-reduced Ag NPs was produced using a modified procedure[42,43] with the conditions specified by Munro et al. Briefly, 200 mL aqueous solution of 10^{-3} M $AgNO_3$ was boiled under vigorous stirring, then 5 mL of 35 mM sodium citrate solution was added, and the resulting mixture was kept boiling for 1 h. The colloidal solution was stored at 4 °C and protected from room light. Before DNA loading, the thiol functionality on the probes was deprotected by treatment with 1.7 equivalents of Tris(2-carboxyethyl)phosphine (TCEP) for 1 h by using acetate buffer (0.05 mM, pH 5.2) at room temperature. The Ag NPs (3 mL, 3.5 nM) were functionalized with the deprotected thiololigonucleotides by incubation at room temperature for at least 16 h with gently stirring and an additional 24 h after the concentration of NaCl had been increased to 100 mM. Then, the excess of DNA was removed by centrifugation (12 000 rpm, 30 min) and redispersed in 10 mM PBS containing 0.1 M NaCl, which was repeated for further purification. The obtained bio-bar-coded nanoparticle probe was redispersed in 1 mL of 10 mM pH 7.4 PBS and stored at 4 °C.

2.4 Immobilization of the capture probe MB.

The process for constructing the electrochemical DNA biosensor is illustrated in Scheme 1. Before modification, a gold electrode (GE) with 3-mm diameter was polished to a mirror using 1.0, 0.3, and 0.05 μm alumina slurry followed by rinsing thoroughly with deionized water. 100 μL of 100 μM thiolated MB1 was incubated with 0.1 μL of 100 mM TCEP for 1 h to reduce disulfide bonds and subsequently diluted to 1.0 μM with phosphate buffer. Then, 5 μL MB (1.0 μM) was dropped on

the GE for 2 h to covalently immobilize the 5-SH modified MB at room temperature in the dark. After rinsing with distilled water, the modified GE was incubated with with the blocking buffer for 1 h at room temperature. The DNA biosensor was obtained after washing 10 mM PBS buffer solution.

2.5 RCA reaction and Ag NPs tagging.

The MB probe-modified electrode was exposed in a series of 10 μL the mixture of target DNA of different concentrations and 5 units Exo III for 0.5 h. After washed with washing buffer, 10 μL of 1 μM padlock probe and 10 μL of 1 μM primer were mixed in 98 μL of ligation buffer and incubated at 37 °C for 30 min. Then, 2 μL of T4 DNA ligase (5 U/μL) was added and incubated at 22 °C for 1 h. After ligation, T4 DNA ligase was inactivated by heating. Then the electrode was incubated with 100 μL RCA reaction buffer containing RCA template (0.1 μM), Phi29 DNA polymerization (8.0 U), dNTPs (0.4 mM) at 37 °C for 2.5 h. After RCA reaction, the solution was removed from the surface of the electrode. The above electrode was immerged in 100 μL of detection probe-modified Ag NPs for 1 h at 37 °C. The electrode was then washed three times with buffer subsequently.

2.6 Measurement Procedure.

Electrochemical experiments were carried out using the CHI 660C electrochemical analyzer. After Ag NPs tagging, the electrode was rinsed with water, and linear sweep voltammetry (LSV) from -0.15 to 0.25 V at 50 mV s^{-1} was performed in a 1.0 M KCl solution. The electrochemical impedance spectroscopy (EIS) measurement was also carried out with the CHI 660C electrochemical analyzer. Supporting electrolyte

solution was 1.0 mmol/L $K_3[Fe(CN)_6]/K_4[Fe(CN)_6]$ (1:1) solution containing 0.1 mol/L KCl. The ac voltage amplitude was 5 mV, and the voltage frequencies used for EIS measurements ranged from 100 kHz to 100 mHz. The applied potential was 172 mV vs. Ag/AgCl[47]. This potential is near the equilibrium of $[Fe(CN)_6]^{3-/4-}$ pair, and makes the redox rates equal. Therefore, the redox species will not be depleted near the electrode surface during the measurement[48]. Tapping mode atomic force microscopic (AFM) image was acquired under ambient conditions using an Agilent 5500 AFM/SPM system.

2.7 Gel electrophoresis.

A 20% non-denaturing polyacrylamide gel electrophoresis (PAGE) analysis of the products was carried out in 1× TBE (pH=8.3) at 80 V constant voltage for about 3 h. After Sybr green I staining, gels were scanned using an Image Master VDS-CL (Amersham Biosciences).

3. Result and discussion

Scheme 1

3.1. Design of electrochemical biosensor.

In order to realize the sensitive detection of target DNA, the cascade signal amplification was performed with Exo III assistant DNA recycling, RCA, Ag NPs tagging, and electrochemical analysis. As shown in Scheme 1, MB probe with a 3′ overhang end was immobilized on the surface of GE, followed by reacting with the target DNA firstly hybridized with specifically designed capture MB to form double-stranded structure, which had unique characteristic 3′-blunt end at the capture

MB and 3′-overhangend at target DNA. Thus Exo III could recognize the formed structure to catalyze the stepwise removal of mononucleotides from 3′-hydroxyl termini of DNA duplexes with 3′-blunt or recessed, which digested the capture MB strand and led to the release of target DNA. The released target DNA hybridized with other capture DNA to trigger the cleavage of MB substrates for formation of numerous MB fragments. After Exo III-assisted target recycling amplification, the capture MB fragments remained on sensor, which can be as a prime for initiating the RCA reaction. After binding RCA template, dNTPs and polymerase were introduced to initiate the RCA reaction. Subsequently, the detection probe modified Ag NPs, whose sequence was complementary to the RCA product in each repeat sequence, were added to hybridize with the long amplified DNA products, resulting in the multiplication of the reporter Ag NPs on the electrode surface. Then, the Ag NPs analyzed by linear sweep voltammetry could avoid the requirement of deoxygenation, which makes the electrochemical detection of DNA simple and sensitivity.

Fig.1

3.2. Verification of the amplified DNA detection method.

First of all, it is essential to confirm the RCA as expected for amplification of DNA detection signal. As shown in Fig. 1A, in the absence of target, the silver electrochemical stripping peak for the mixture of Exo III, RCA template, polymerase and dNTPs (curve b) was slight larger than the blank (curve a) due to the non-specific adsorption of Ag NPs reporters on the GE surface, but so smaller than the presence of target DNA (curve d), indicating that no RCA reaction was triggered. In the presence

of target and Exo III, the recognition of MB modified electrode to 10 fmol L^{-1} DNA after RCA process led to an obvious stripping peak (curve d), which was greater than that before RCA (curve c), showing obvious signal amplification. Thus the DNA target could hybridize with the immobilized MB and the cleavage of a large number of the MB with Exo III. Then, the left MB fragment as a prime hybridizes with the RCA template to initiate the RCA process. The obtained RCA product was a long single-strand DNA containing thousands of repeated sequences for linear periodic hybridization with Ag NPs.

In order to further verify that no RCA reaction was triggered in the absence of target, hybridization tests using free DNA strands in solution were performed (ESI†, Scheme S1). A fluorophore and a quencher were added on the fluorescent probe. As shown in Fig. S1 (ESI†), by itself or in the absence of target DNA, no fluorescence response was observed (ESI†, Fig. S1, curve a). However, upon addition of target DNA, an enhanced fluorescence peak was observed (ESI†, Fig. S1, curve b), indicates that only the target DNA could trigger RCA reaction.

PAGE analysis was also used to investigate the viability of the sensing strategy (Fig. 1B). The MB showed only one band (lane a) at the position different from the mixture of MB, and target (lane b). The difference resulted from the hybridization of MB with target in the mixture. The formed dsDNA produced a new band. Upon addition of Exo III to the mixture, the band corresponding to the double stranded disappeared and two new bands were observed at a longer distance, while the later band corresponding to target DNA occurred (lane c) and the faster corresponding to the MB fragments. After

the RCA template, polymerase and dNTPs were added, a new band appear (lane d) with a slower migration rate than lane c, which should be attributed to the obtained RCA product containing thousands of repeated sequences. The PAGE data demonstrated the feasibility of the designed strategy.

Fig.2

3.3. Characterzation of the modifying process.

EIS was carried out to study the modification of the electrode surface. The typical electrochemical interface can be represented as an electrical circuit as shown in the inset of Fig. 2 (Randles and Ershler theoretical model). The equivalent circuit includes four parameters. The ohmic resistance of the electrolyte solution, Rs, the Warburg impedance, Zw, represent bulk properties of the electrolyte solution and diffusion features of the redox probe in solution. The double-layer capacitance, CPE, and the charge -transfer resistance, Rct, reveal interfacial properties of the electrode, which is highly sensitive to the surface modification. Usually, Rct controls the interfacial electron-transfer rate of the redox probe between the solution and the electrode. In the Nyquist plot of impedance spectroscopy, Rct at the electrode surface is equal to the semicircle diameter. As show in Fig.2, the impedance plot for the bare electrode exhibited a very small semicircle (curve a), which suggested a low electron transfer resistance. After the DNA capture probe was modified on the electrode surface caused a further increase in the electron transfer impedance (curve b), since the negative charge on the phosphate backbone of DNA interfered with the movements of $[Fe(CN)_6]^{3-/4-}$ ion. In the presence of target, recognition probes hybridized with

capture probes, which led to the increase of faraday impedance (curve c). The Ret decreased significantly (curve d) when the biosensor was hybridized with target DNA and reacted with Exo III, which was attributed to the fact that considerable capture DNA strands were digested, which proved the successful implement of Exo III-assisted target recycling amplification. After RCA, the impedance increases significantly (curve e) because of long amplified DNA products were captured on the electrode surface, which made the electron transfer become more difficult. After Ag NPs reporters were modified on the electrode surface, the resistance decreased (curve f), which is attributed to the fact that Ag NPs could significantly enhance the effective surface area of the electrode to facilitate the electron transfer.

The density of immobilized MB on the gold electrode could affect the analytical performance of the sensor. In order to know the surface density of MB, RuHex cation has been well explored as an electrochemical indicator to quantitatively bind to the phosphate backbone of DNA via electrostatic interaction. As shown in Fig. S2A (ESI†), RuHex binding to MB modified GE can induce greater electrochemical signal compare with blank GE. The surface coverage of MB under the optimum condition had also been determined on the basis of Tarlov's method[49]. It was estimated to be 4.43×10^{12} mol cm^{-2} based on three independent experiments. Notably, the grafting efficiency is closely related to the length and structure of the capture probe used for the reaction. AFM was also used to characterize the morphology of MB on GE surface. As shown in Fig. S2 (ESI†), a monolayer of MB tightly packed on the GE surface. Furthermore, the AFM data shows that the height of the immobilized MB

varied from 8 to 10 nm, which was very close to the theoretically calculated value (9.1 nm) for 27 bases (half length of MB) of length 0.34 nm each base, indicating that some DNA molecules lay flat while others stood vertically on the surface.

Fig.3

3.4. Optimization of detection conditions.

In this paper, the detection conditions were affected by six factors including the amount of dNTPs, Exo III, polymerase, Ag NPs reporters, and the reaction time of Exo III assisted DNA recycling and RCA. As shown in Fig. 3A, B, C, and D, the current intensity of stripping response increased with the increasing amount of dNTPs, Exo III, polymerase, and the volume of Ag NPs, then trended a maximum value, indicating a saturated amplification. The optimal amount of dNTPs, Exo III, polymerase and Ag NPs were selected at 2.5 mM, 5 U, 8 U and 80 μL, respectively. As we all know, the current was dependent on the amount of the Ag NPs bound to the RCA product. The greater the number of MB fragment produced by Exo III, the greater the number of long RCA products DNA. The greater the number of repeated sequences produced by RCA reaction, the greater the amount of Ag NPs bound on the electrode. In theory, a long RCA reaction time was expected to generate more repeated sequences. As shown in Fig. 3E and 3F, the current intensity increased rapidly with the time of the reaction duration trended to a constant value. Thus the optimal reaction time of Exo III and RCA were chosen as 30 min and 2.5 h, respectively.

Fig.4

3.5. Sensitivity of the DNA biosensor.

At optimal conditions, the DNA assay was challenged with a series of target DNA concentration. As shown in Fig. 4, the peak of stripping current increased as the concentration of the target DNA increase. It was found that the response signal was logarithmically proportional to the target concentration in the range from 10 aM to 1.0 pM. The linear calibration equation was I = 157.72 + 9.03 log C (I is the peak current (μA) and C is the concentration of the target DNA (mol L^{-1})) and the correlation coefficient R^2=0.9913. The limit of detection (LOD) was 6.4 amol L^{-1} according to the 3σ rule (where σ is the standard deviation of the blank)[54]. We use 3σ as I, and put it into the formula (I = 157.72 + 9.03 log C) for calculating the C, the C was LOD. Compared to other electrochemical methods, this proposed method showed a lower limit of detection, and was competitive with the highly sensitive detection of DNA by PCR technique[50]. In addition, this method was superior to some amplification techniques, such as target cycling-based amplification (0.167 pM)[51], bio-barcodes (2.5 fM)[52] and Au NPs-based amplification (10 zmol)[53]. Thus the high sensitivity of this method was mainly attributed to the amplification of Exo III assisted DNA recycling and RCA process, which made many of Ag NPs reporters modify on the surface of GE.

Fig.5

3.6. Selectivity of the DNA biosensor.

The selectivity of the DNA biosensor based on exonuclease III assisted DNA recycling and rolling circle amplification was studied by using three kinds of DNA sequence with concentrations of 10.0 fmol L^{-1} including perfectly complementary

target, one-base mismatched strand and non-complementary strand. The comparison of the three responses and background is shown in Fig. 5. The perfectly complementary target shows a response 12.7 times that of the single-base mismatch sequence, indicating good selectivity. The response of the non-complementary strand is only 5.8% that of the perfectly complementary target, which mainly results from the hairpin structure thermodynamically stable, and being unfavorable for the hybridization between mismatched sequences and MB. These results demonstrate that the electrochemical DNA biosensor is able to detect effectively a target with high specificity, and has great potential for single nucleotide polymorphism analysis. Meanwhile, the proper position of the base mismatch site and the low concentrations of the two kinds of DNA molecules also contributed to the high selectivity.

3.7 Reproducibility for target DNA detection.

The reproducibility of the suggested electrochemical detection method was examined by six repetitive measurements of 1.0 fM target DNA on a single electrode, which showed a relative standard deviation (RSD) of 3.4%. The RSD for ten parallel DNA sensors fabricated on different electrode was 4.9%. These results indicated the satisfactory reproducibility for both DNA detection and DNA sensor fabrication.

3.8 Application in real sample.

To test the generality of the proposed assay in the clinical sample, recovery testing was carried out by spiking target DNA solution into human serum. At the concentration of 1.0 pM and 0.1 fM, the recoveries were 95.4 ± 1.9% and 95.3 ± 2.3% (n=5), indicating that the proposed strategy for DNA detection could be used in real

sample analysis.

4. Conclusions

In this paper, a novel electrochemical method for detecting DNA hybridization was developed based on dual amplification of Exo III assisted DNA recycling and rolling circle amplification. This method has significant advantages of improved sensitivity and high selectivity. The detection limit of this method is 6.4 amol L^{-1}, and the detectable concentration was in a linear range of 5 orders of magnitude, which is attributed to a very low background signal and large signal enhancement. The excellent selectivity to differentiate single-base mismatched sequences of DNA was verified due to the intrinsic functions of MB and polymerase. The electrochemical oxidation of Ag NPs in KCl excluded specific detection conditions, such as pretreatment of the NPs, high stripping potential, and deoxygenation procedure. This strategy of cascade signal amplification could be extended to other analytical techniques by changing the signal tag. Therefore, the method presented a potential tool for early diagnosis of gene related disease and represents an attractive alternative to indirect affinity assays of antibodies and other biomolecules.

Acknowledgment

This work was supported by the National Natural Science Foundation of China (21405130, 21264001), Excellent Talents by Xuzhou Medical College (D2014007).

References

1. J. M. Kong, A. R. Ferhan, X. T. Chen, L. Zhang and N. Balasubramanian, *Anal. Chem.*, 2008, **80**, 7213–7217.

2. Q. Hu, W. W. Hu, J. M. Kong and X. J. Zhang, *Biosens. Bioelectron.*, 2015, **63**, 269–275.

3. P. He, W. P. Qiao, L. J. Liu and S. S. Zhang, *Chem. Commun.*, 2014, **50**, 10718–10721.

4. Y. Chen, J. Xu, J. Su, Y. Xiang, R. Yuan and Y. Q. Chai, *Anal. Chem.*, 2012, **84**, 7750–7755.

5. S. F. Liu, C. F. Wang, C. X. Zhang, Y. Wang and B. Tang, *Anal. Chem.*, 2013, **85**, 2282–2288.

6. S. F. Liu, Y. Lin, T. Liu, C. B. Cheng, W. J. Wei, L. Wang and F. Li, *Biosens. Bioelectron.*, 2014, **56**, 12–18.

7. T. Hou, X. J. Liu, X. Z. Wang, A. W. Jiang, S. F. Liu and F. Li, *Sensor Actuat. B–Chem.*, 2014, **190**, 384–388.

8. J. C. Cunningham, N. J. Brenes and R. M. Crooks, *Anal. Chem.*, 2014, **86**, 6166–6170.

9. P. Liu, X. H. Yang, S. S. Sun, Q. Wang, K. M. Wang, J. Huang, J. B. Liu and L. L. He, *Anal. Chem.*, 2013, **85**, 7689–7695.

10. C. P. Ma, W. S. Wang, A. Mulchandani and C. Shi, *Anal. Biochem.*, 2014, **457**, 19–23.

11. A. Baeissa, N. Dave, B. D. Smith and J. W. Liu, *ACS Appl. Mater. Interfaces*, 2010, **2**, 3594–3600.

12. J. Thavanathan, N. M. Huang and K. L. Thong, *Biosens. Bioelectron.*, 2014, **55**, 91–98.

13. Y. J. Song, X. H. Wang, C. Zhao, K. G. Qu, J. S. Ren and X.G. Qu, *Chem. Eur. J.*,

2010, **16**, 3617–3621.

14. S. F. Liu, Y. Lin, L. Wang, T. Liu, C. B. Cheng, W. J. Wei and B. Tang, *Anal. Chem.*, 2014, **86**, 4008–4015.

15. H. Y. Liu, L. Li, Q. Wang, L. L. Duan and B. Tang, *Anal. Chem.*, 2014, **86**, 5487–5493.

16. S. F. Liu, Y. Wang, J. J. Ming, Y. Lin, C. B. Cheng and F. Li, *Biosens. Bioelectron.*, 2013, **49**, 472–477.

17. Z. P. Zhang, J. Y. Zhou, A. Tang, Z. Y. Wu, G. L. Shen and R. Q. Yu, *Biosens. Bioelectron.*, 2010, **25**, 1953–1957.

18. H. Zhang, C. C. Fang and S. S. Zhang, *Chem. Eur. J.*, 2010, **16**, 12434–12439.

19. M. S. Wu, L. J. He, J. J. Xu and H. Y. Chen, *Anal. Chem.*, 2014, **86**, 4559–4565.

20. M. Li, Y. H. Wang, Y. Zhang, J. H. Yu, S. G. Ge and M. Yan, *Biosens. Bioelectron.*, 2014, **59**, 307–313.

21. G. F. Jie, J. Zhang, G. X. Jie and L. Wang, *Biosens. Bioelectron.*, 2014, **52**, 69–75.

22. H. F. Zhao, R. P. Liang, J. W. Wang, and J. D. Qiu, *Biosens. Bioelectron.*, 2015, **63**, 458–464.

23. G. J. Zhang, Z. H. H. Luo, M. J. Huang, G. K. I. Tay and E. A. Lim, *Biosens. Bioelectron.*, 2010, **25**, 2447–2453.

24. B. J. Cai, S. T. Wang, L. Huang, Y. Ning, Z. Y. Zhang and G. J. Zhang, *ACS Nano*, 2014, **8**, 2632–2638.

25. S. W. Bae, M. S. Cho, S. S. Hur, C. B. Chae, D. S. Chung, W. S. Yeo and J. I. Hong, *Chem. Eur. J.*, 2010, **16**, 11572–11575.

26. X. Wang, X. H. Lou, Y. Wang, Q. C. Guo, Z. Fang, X. H. Zhong, H. J. Mao, Q. H.

Jin, L. Wu, H. Zhao and J. L. Zhao, *Biosens. Bioelectron.*, 2010, **25**, 1934–1940.

27. E. S. Jeng, J. D. Nelson, K. L. J. Prather and M. S. Strano, *Small*, 2010, **6**, 40–43.

28. S. F. Liu, C. B. Cheng, T. Liu, L. Wang, H. W. Gong and F. Li, *Biosens. Bioelectron.,* 2015, **63**, 99–104.

29. C. F. Zhu, Z. Y. Zeng, H. Li, F. Li, C. H. Fan and H. Zhang, *J. Am. Chem. Soc.*, 2013, **135**, 5998–6001.

30. Z. Gao, S. Rafea and L. H. Lim, *Adv. Mater.*, 2007, **19**, 602–606.

31. J. Wang, D. K. Xu and R. Polsky, *J. Am. Chem. Soc.*, 2002, **124**, 4208–4209.

32. G. Liu, Y. Wan, V. Gau, J. Zhang, L. H. Wang, S. P. Song and C. H. Fan, *J. Am. Chem. Soc.*, 2008, **130**, 6820–6825.

33. H. Li, Z. Y. Sun, W. Y. Zhong, N. Hao, D. K. Xu and H. Y. Chen, *Anal. Chem.*, 2010, **82**, 5477–5483.

34. J. Zhang, B. P. Ting, N. R. Jana, Z. Q. Gao and J. Y. Ying, *Small*, 2009, **5**, 1414–1417.

35. H. Deng, Y. Xu, Y. H. Liu, Z. J. Che, H. L. Guo, S. X. Shan, Y. Sun, X. F. Liu, K. Y. Huang, X. W. Ma, Y. Wu and X. J. Liang, *Anal. Chem.*, 2012, **84**, 1253–1258.

36. W. Y. Zhang, W. H. Zhang, Z. Y. Liu, C. Li, Z. Zhu and C. Y. J. Yang, *Anal. Chem.*, 2012, **84**, 350–355.

37. J. Li, B. Yao, H. Huang, Z. C. Wang, Sun, H. Y. Fan, Q. S. Chang, L. Li, X. Wang and J. Z. Xi, *Anal. Chem.*, 2009, **81**, 5446–5451.

38. S. Bi, J. L. Zhang, and S. S. Zhang, *Chem. Commun.*, 2010, **46**, 5509–5511.

39. Z. Y. Liu, W. Zhang, S. Y. Zhu, L. Zhang, L. Z. Hu, S. Parveen and G. B. Xu, *Biosens. Bioelectron.*, 2011, **29**, 215–218.

40. X. L. Zuo, F. Xia, Y. Xiao and K. W. Plaxco, *J. Am. Chem. Soc.*, 2010, **132**, 1816–1818.

41. C. Q. Zhao, L. Wu, J. Ren and X. G. Qu, *Chem. Commun.*, 2011, **47**, 5461–5463.

42. S. B. Zhang, Z. S. Wu, G. L. Shen and R. Q. Yu, *Biosens. Bioelectron.*, 2009, **24**, 3201–3207.

43. J. L. He, Z. S. Wu, H. Zhou, H. Q. Wang, J. H. Jiang and G. L. Shen, R. Q. Yu, *Anal. Biochem.*, 2010, **82**, 1358–1364.

44. M. M. Ali and Y. F. Li, *Angew. Chem. Inter. Edit.*, 2009, **48**, 3512–3515.

45. P. C. Lee and D. J. J. Meisel, *Chem. Phys.*, 1982, **86**, 3391–3395.

46. C. H. Munro, W. E. Smith, M. Garner, J. Clarkson and P. C. White, *Langmuir*, 1995, **11**, 3712–3720.

47. W. Zhang, T. Yang, X. M. Zhuang, Z. Y. Guo and K. Jiao, *Biosens. Bioelectron.*, 2009, **24**, 2417–2422.

48. S. L. Pan and L. Rothberg, Langmuir 2005, **21**, 1022–1027.

49. A. B. Steel, T. M. Herne and M. J. Tarlov, *Anal. Chem.*, 1998, **70**, 4670–4677.

50. A. Ramanaviciene and A. Ramanavicius, *Anal. Bioanal. Chem.*, 2004, **379**, 287–293.

51. Z. Y. Liu, W. Zhang, S. Y. Zhu, L. Zhang, L. Z. Hu, S. Parveen and G. B. Xu, *Biosens. Bioelectron.*, 2011, **29**, 215–218.

52. H. D. Hill, R. A. Vega and C. Mirkin, *Anal. Chem.*, 2007, **79**, 9218–9223.

53. S. Pinijsuwan, P. Rijiravanich, M. Somasundrum and W. Surareungchai, *Anal. Chem.*, 2008, **80**, 6779–6784.

54. L. E. Vanatta and D. E. Coleman, *J. Chromatogra. A*, 1997, **770**, 105–114.

Figure captions:

Scheme 1 Schematic representation of electrochemical detection of DNA based on Exo III assisted DNA recycling and RCA for dual signal amplification.

Fig. 1 LSV curves of Ag NPs deposited at sensor surface (50 mV s^{-1} in 1.0 M KCl) in the presence of (a) blank, (b) RCA template, dNTPs and polymerase, (c) 10 fmolL^{-1} target, Exo III, (d) (c) + RCA template, dNTPs and polymerase. (B) PAGE analysis of the products via the isothermal RCA with (a) 10^{-7} M MB, (b) 10^{-7} M MB and 10^{-7} M target; (c) 10^{-7} M MB, 10^{-7} M RCA template and 10^{-7} M target; (d) (c) in the presence of polymerase and dNTPs.

Fig. 2 EIS in 0.1M KNO_3 containing 5 mM $K_3[Fe(CN)_6]/K_4[Fe(CN)_6]$ at (a) bare GE, (b) immobilization of MB, (c) hybridization with target sequence, (d) (c) + 5 U Exo III, (e) (d) + in the presence of RCA template, polymerase and dNTPs, and (f) (d) + attaching of Ag NPs.

Fig. 3 Dependence of current intensity for 10 fmol L^{-1} targets DNA on (A) the amount of dNTPs, (B) Exo III, and (C) polymerase, (D) the volume of Ag NPs, the reaction time of (E) Exo III assisted DNA recycling and (F) RCA. When one parameter changes the others are under their optimal conditions (n=5).

Fig. 4 (A) LSV curves of the DNA sensors toward target DNA with various concentrations of 10^{-18}–10^{-12} mol L^{-1} (a to g) in 1.0 M KCl by using silver nanotags as reporters, (B) the corresponding calibration curve (n=5).

Fig. 5 Histograms of current intensity for 1.0 fmol L^{-1} (a) complementary, (b) single-base mismatched, (c) non-complementary sequences, and (d) blank (n=5).

Scheme 1

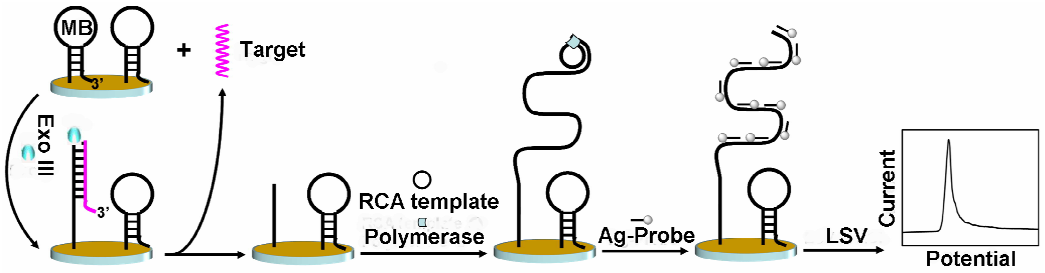

Fig.1

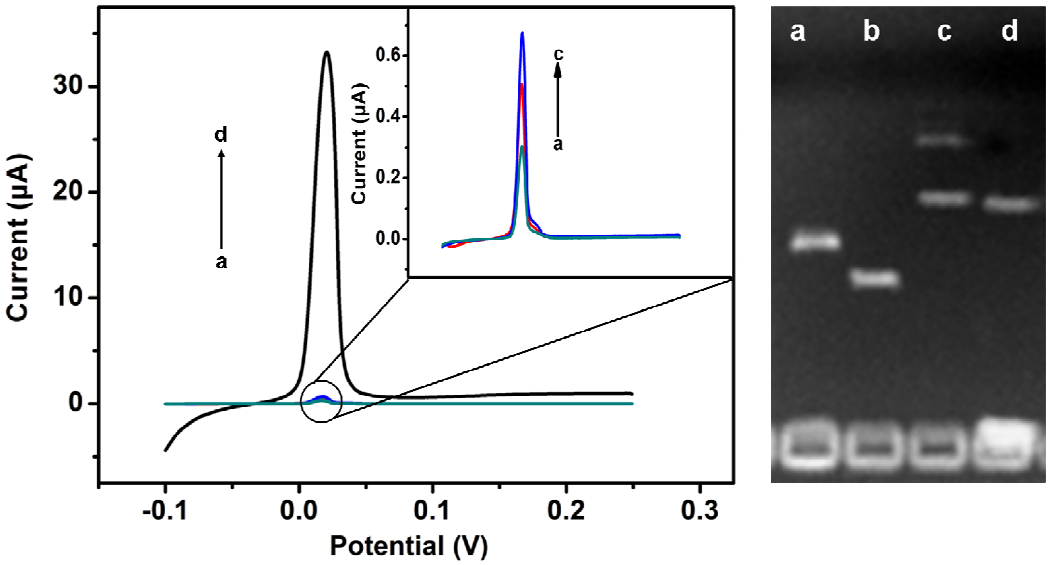

Fig.2

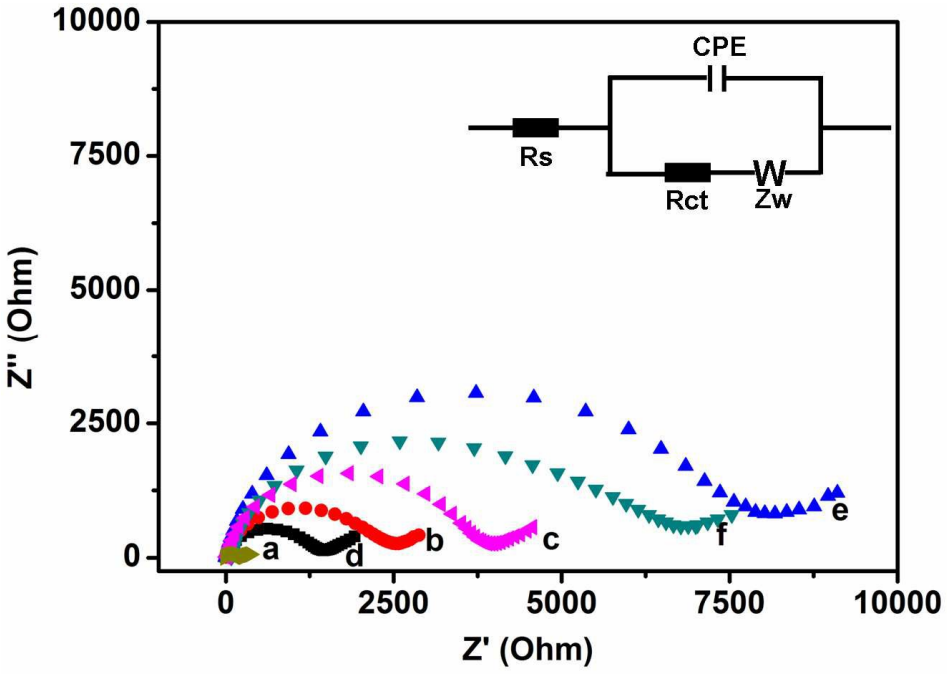

Fig.3

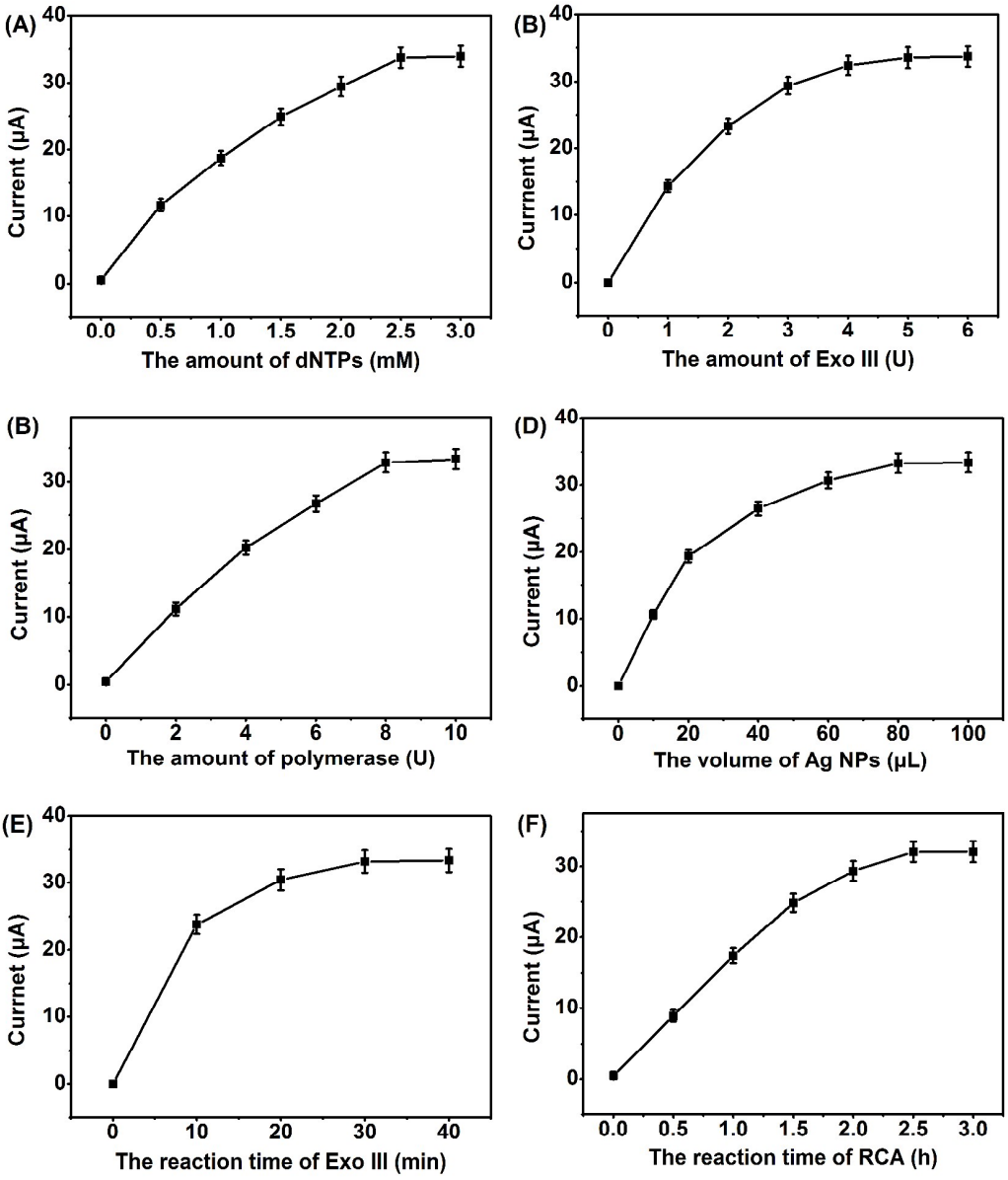

Fig.4

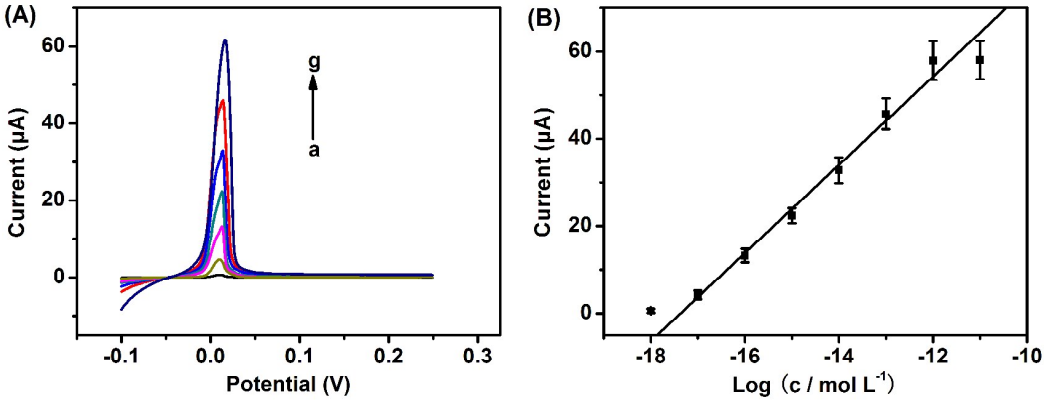

Fig.5